

Spatial control in the heterogeneous nucleation of water

Kripa K. Varanasi¹, Ming Hsu, Nitin Bhate, Wensha Yang, and Tao Deng¹

Citation: *Appl. Phys. Lett.* **95**, 094101 (2009); doi: 10.1063/1.3200951

View online: <http://dx.doi.org/10.1063/1.3200951>

View Table of Contents: <http://aip.scitation.org/toc/apl/95/9>

Published by the [American Institute of Physics](#)

Articles you may be interested in

[Frost formation and ice adhesion on superhydrophobic surfaces](#)

Appl. Phys. Lett. **97**, 234102234102 (2010); 10.1063/1.3524513

[Dropwise condensation on superhydrophobic surfaces with two-tier roughness](#)

Appl. Phys. Lett. **90**, 173108173108 (2007); 10.1063/1.2731434

[Visualization of droplet departure on a superhydrophobic surface and implications to heat transfer enhancement during dropwise condensation](#)

Appl. Phys. Lett. **97**, 033104033104 (2010); 10.1063/1.3460275

[Condensation heat transfer on two-tier superhydrophobic surfaces](#)

Appl. Phys. Lett. **101**, 131909131909 (2012); 10.1063/1.4756800



NEW 8600 Series VSM
For fast, highly sensitive
measurement performance

[LEARN MORE ▶](#)

Spatial control in the heterogeneous nucleation of water

Kripa K. Varanasi,^{1,a),b)} Ming Hsu,² Nitin Bhate,² Wensha Yang,² and Tao Deng^{2,a),c)}

¹*Department of Mechanical Engineering, Massachusetts Institute of Technology, Cambridge, Massachusetts 02139, USA*

²*Nanotechnology Advanced Technology, GE Global Research Center, Niskayuna, New York 12309, USA*

(Received 29 June 2009; accepted 9 July 2009; published online 31 August 2009)

Heterogeneous nucleation of water plays an important role in a wide range of natural and industrial processes. Though heterogeneous nucleation of water is ubiquitous and an everyday experience, spatial control of this important phenomenon is extremely difficult. Here we show for the first time that spatial control in the heterogeneous nucleation of water can be achieved by manipulating the local nucleation energy barrier and nucleation rate via the modification of the local intrinsic wettability of a surface. Such ability to control water nucleation could address the condensation-related limitations of superhydrophobic surfaces and has implications for efficiency enhancements in energy and desalination systems. © 2009 American Institute of Physics. [DOI: 10.1063/1.3200951]

Heterogeneous nucleation of water is an everyday phenomenon and plays an important role in the formation of rain drops, dew, heat transfer, steam nucleation in power turbines, aerosol detection, water recovery, desalination, etc. Classical nucleation theory predicts that an energy barrier that depends strongly on the intrinsic wettability of the surface has to be overcome for the formation of initial liquid nuclei on the surface.¹ Since the intrinsic wettability of regular surfaces is spatially uniform, heterogeneous nucleation of water droplets occurs in a random fashion without any particular spatial preference. This effect accounts for the recent observations on the loss of superhydrophobic properties of lotus leaves^{2,3} and associated synthetic surfaces under condensation^{4–6} and has been identified as a critical limitation of superhydrophobic surfaces.⁷ By taking advantage of the strong dependence of the nucleation energy barrier and nucleation rate on wettability, we report here for the first time that heterogeneous nucleation can be spatially controlled by the manipulation of the local intrinsic wettability of a surface. Using an environmental scanning electron microscope (ESEM), we show that water droplets preferentially nucleate on the hydrophilic regions of hybrid hydrophobic-hydrophilic surfaces we fabricated. This ability to control nucleation-level phenomena can be used to overcome condensation-related limitations of superhydrophobic surfaces and has implications for enhancing heat and mass transport.

Condensation of water vapor from moist air and steam has been an active area of research for more than a century.⁸ According to Volmer's classical nucleation theory,¹ the free energy barrier ΔG for the formation of a liquid nucleus on a flat surface depends strongly on the intrinsic wettability of the surface via the contact angle θ ,

$$\Delta G = \pi\sigma_{lv}r^*(2 - 3 \cos \theta + \cos^3 \theta)/3, \quad (1)$$

where σ_{lv} is the liquid-vapor surface energy and r^* is the critical radius. The formula for the critical radius is given by Kelvin's classical equation $\ln(p/p_\infty) = 2\sigma_{lv}/n_l kTr^*$, where p

is the vapor pressure over a curved interface of radius r^* , p_∞ is the equilibrium vapor pressure above a flat surface of the condensed phase at temperature T , n_l is the number of molecules per unit volume of the liquid, and k is the Boltzmann constant. The intrinsic wettability of the surface has a strong effect on the nucleation rate J via the inverse exponential dependence on ΔG ,

$$J = J_o \exp(-\Delta G/kT) = J_o \exp[\pi\sigma_{lv}r^*{}^2(2 - 3 \cos \theta + \cos^3 \theta)/3kT], \quad (2)$$

where J_o is a kinetic constant. Therefore, a surface with spatially uniform intrinsic wettability will be characterized by a spatially uniform ΔG and J , and as a result heterogeneous nucleation on such surfaces occurs without any particular spatial preference as a random process. This phenomenon was evident in our ESEM study of water vapor condensation on a superhydrophobic surface comprising of an array of hydrophobic silicon posts as shown in Fig. 1 (and in movie 1).⁹ Because of the spatially uniform intrinsic wettability of the surface,¹⁰ ΔG and J are also spatially uniform resulting in droplet nucleation all over the post surfaces (post tops, side walls, and valleys). This nonpreferential nucleation results in the formation of a mixture of Cassie-type and Wenzel-type droplets under condensation, in contrast to the usually observed Cassie behavior in the case of sessile^{10,11} and bouncing droplets¹² on such surfaces. This nucleation-driven phenomenon results in the loss of the metastable non-wetting states on textured hydrophobic surfaces, accounts for the observed loss of superhydrophobic properties of lotus leaves and lotus-inspired surfaces, and renders them ineffective under condensation.^{2–7}

The question that naturally arises is: can one achieve spatial control in the heterogeneous nucleation of water? If this spatial control were possible, droplets can be made to preferentially nucleate on post tops, thereby forcing Cassie-type behavior on textured surfaces even under condensation. Such an approach can result in superior droplet shedding surfaces even in condensation environments and lead to high-quality dropwise condensation since Cassie droplets have lower hysteresis. One possible approach to answer this

^{a)} Authors to whom correspondence should be addressed.

^{b)} Electronic mail: varanasi@mit.edu. Tel.: 617-324-5608.

^{c)} Electronic mail: dengt@research.ge.com. Tel.: 518-387-5473.

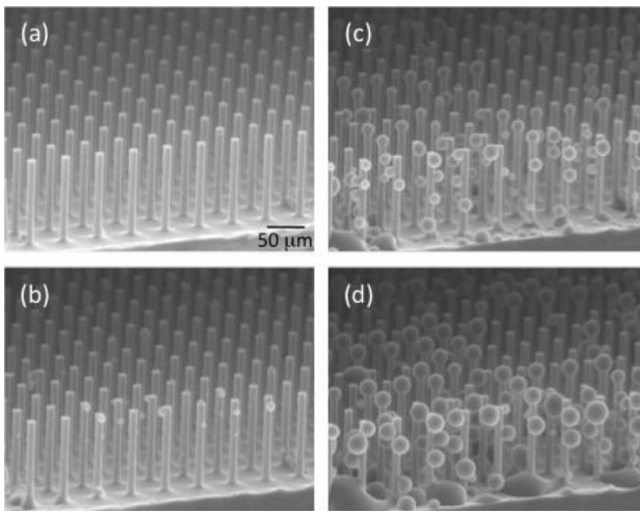


FIG. 1. ESEM images of the condensation of water vapor on a superhydrophobic surface comprising of an array of hydrophobic square posts with width, edge-to-edge spacing, and aspect ratio of $15\ \mu\text{m}$, $30\ \mu\text{m}$, and 7, respectively. (a) Dry surface. [(b)–(d)] Snapshot images of the condensation phenomenon on the surface. The intrinsic contact angle of the hydrophobic coating on the posts is $\sim 110^\circ$. The surface is maintained at a temperature of 274 K by means of a cold stage accessory of the ESEM. At the beginning of the experiment, the chamber pressure is maintained at $\sim 400\ \text{Pa}$, well below the saturation pressure to ensure a dry surface. The vapor pressure in the chamber is then slowly increased until droplet nucleation is observed. Droplet nucleation occurs without any particular spatial preference due to the uniform intrinsic wettability of the surface. These droplets grow and coalesce and would ultimately result in a mixture of Cassie- and Wenzel-type droplets. An ESEM video of the phenomenon is provided in movie 1 (see Ref. 9).

question lies in the dependence of ΔG and J on θ as given by Eqs. (1) and (2). The nucleation energy barrier continuously increases with contact angle, indicating that hydrophobic surfaces have higher ΔG when compared to hydrophilic surfaces under identical conditions (see Fig. S1 in Ref. 9). For example, the ΔG for a hydrophobic surface with a $\theta \sim 110^\circ$ would be about 117 times higher than that of a hydrophilic surface with a $\theta \sim 25^\circ$. Consequently, the nucleation rate on the hydrophilic surface would be significantly higher than that on the hydrophobic surface due to the inverse exponential dependence of J on ΔG (see Fig. S1 in Ref. 9). An estimate of the nucleation rate for a typical saturation ratio $p/p_\infty = 1.7$ (corresponding to $r^* \sim 2\ \text{nm}$ at $T = 274\ \text{K}$) indicates that the nucleation rate on the hydrophilic surface with $\theta \sim 25^\circ$ is zillions of orders of magnitude ($\sim 10^{129}$ times) higher than that on the hydrophobic surface with a $\theta \sim 110^\circ$. Hence, a surface patterned with hydrophobic and hydrophilic regions that have significant difference in intrinsic wettability can be potentially used to create spatial preference for nucleation, where nucleation would be favored on the hydrophilic regions of the surface. The larger the difference between the intrinsic wettability of these regions, the stronger is the propensity to cause this preference.

To verify this concept, we fabricated two types of hybrid hydrophobic-hydrophilic surfaces⁹ and conducted condensation experiments in an ESEM. The first surface consists of alternating hydrophobic and hydrophilic segments on a silicon wafer with intrinsic contact angles of $\sim 110^\circ$ and $\sim 25^\circ$, respectively. The hydrophilic regions are made up of the native oxide on Si wafer, while the hydrophobic regions are modified with fluorosilane. These segments are $25\ \mu\text{m}$ in

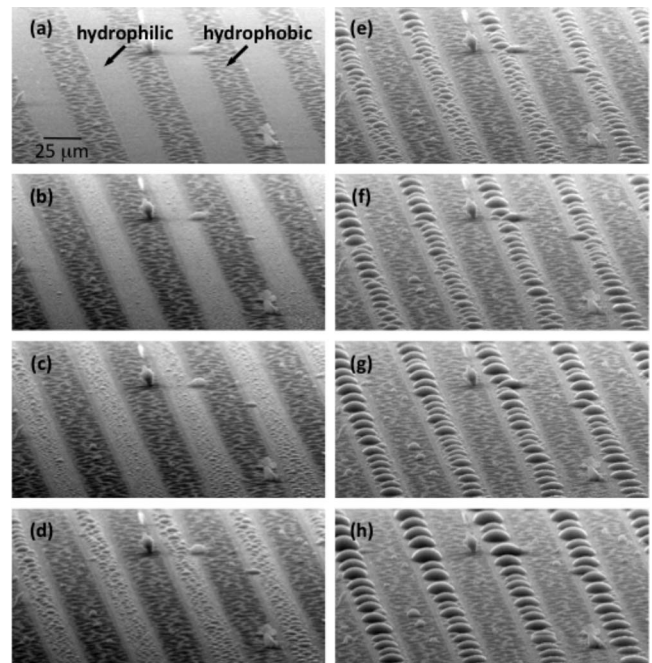


FIG. 2. ESEM images of condensation of water vapor on a surface with alternating hydrophobic and hydrophilic segments. (a) Dry surface. [(b)–(h)] Snapshot images of the condensation phenomenon on the surface. The width of the segments is about $25\ \mu\text{m}$. The intrinsic contact angle of the hydrophilic regions is $\sim 25^\circ$ and that of the hydrophobic regions is $\sim 110^\circ$. The surface was maintained at a temperature of 274 K by means of a cold stage accessory of the ESEM. At the beginning of the experiment, the chamber pressure is maintained at $\sim 400\ \text{Pa}$, well below the saturation pressure to ensure a dry surface. The vapor pressure in the chamber is then slowly increased until droplet nucleation is observed. Droplets are observed to preferentially nucleate and grow on the hydrophilic regions due to the lower ΔG and significantly higher J . An ESEM video of the phenomenon is provided in movie 2 (see Ref. 9).

width and were fabricated via microcontact printing using a prefabricated polydimethylsiloxane stamp.⁹ Condensation experiments were conducted on these surfaces in ESEM and images (taken over a span of 30 s) are shown in Fig. 2 (and in movie 2).⁹ These ESEM images clearly demonstrate that a large difference in the intrinsic wettability of the hydrophilic and hydrophobic segments results in preferential nucleation and subsequent droplet growth on the hydrophilic segments of the hybrid surface.

The second surface is a textured surface consisting of an array of hydrophobic posts with hydrophilic tops. As in the case of the hybrid segments, the intrinsic contact angle of the hydrophobic and hydrophilic regions are $\sim 110^\circ$ and $\sim 25^\circ$, respectively. This hybrid surface was fabricated via lithography combined with UV-assisted surface modification approach.⁹ The hydrophilic tops are made up of deposited silicon dioxide, while the hydrophobic sidewalls and valleys are modified with fluorinated hydrocarbon molecules. The fabrication results were validated by two independent techniques: Time-of-Flight Secondary Ion Mass Spectrometry (ToF-SIMS) and Auger analysis. As shown in Fig. S2 in Ref. 9. ToF-SIMS analysis of the surface revealed that the post sidewalls and valleys were indeed modified to fluorine-rich surfaces, while the post tops remain rich in oxygen. Next, we conducted simultaneous ESEM experiments on such a hybrid surface and a superhydrophobic surface with identical texture. The images from these experiments are shown in Fig. 3 (and in movie 3 and movie 4).⁹ These ESEM images clearly

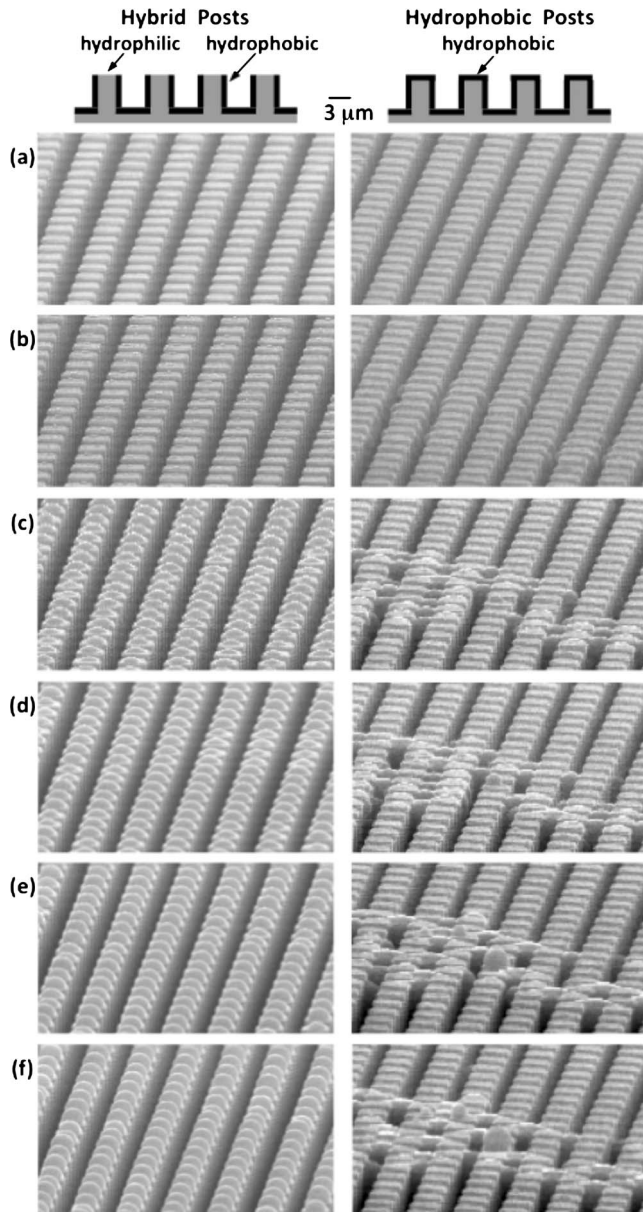


FIG. 3. Comparison of the condensation behavior on a hybrid surface consisting of hydrophobic posts with hydrophilic tops (left) with that of a superhydrophobic surface consisting of hydrophobic posts (right). (a) Dry surface. [(b)–(f)] Snapshot images of the condensation phenomenon on the surfaces. The geometry of the posts is identical for both surfaces with width, edge-to-edge spacing, and aspect ratio of $3\ \mu\text{m}$, $1.5\ \mu\text{m}$, and 3, respectively. The intrinsic contact angle of the hydrophilic regions is $\sim 25^\circ$ and that of the hydrophobic regions is $\sim 110^\circ$. The surfaces were maintained at a temperature of 274 K by means of a cold stage accessory of the ESEM. At the beginning of the experiment, the chamber pressure is maintained at $\sim 400\ \text{Pa}$, well below the saturation pressure to ensure a dry surface. The vapor pressure in the chamber is then slowly increased until droplet nucleation is observed. Droplets are observed to preferentially nucleate and grow on the hydrophilic post tops for the hybrid surface (left), whereas droplets nucleate and grow everywhere without any spatial preference on the superhydrophobic surface (right). ESEM videos of the phenomena are provided in movie 3 and movie 4 (see Ref. 9).

demonstrate that nucleation and subsequent growth of droplets occur preferentially on the hydrophilic post tops of the hybrid surface when compared to the random nucleation of droplets on the identically textured superhydrophobic surface with uniform wettability.

The textured hybrid surface discussed above is reminiscent of the water-capturing surface of the Namib beetle.^{13,14} Our results complement the findings of Parker and Lawrence¹³ and Zhai *et al.*,¹⁴ who suggested that the Namib beetle captures water by collecting small airborne water droplets present in the early morning fog on the hydrophilic regions of its surface. In addition to this mechanism of trapping airborne droplets, we propose that the beetle's surface can capture water by *direct and preferential heterogeneous vapor-to-liquid nucleation* onto the hydrophilic regions on the surface. Subsequently, these droplets grow by further condensation and coalescence and roll into the beetle's mouth. Thus, we believe that the beetle's surface is nature's version of dropwise condensing surface.

In summary, we demonstrate that spatial control in the heterogeneous nucleation of water can be achieved. Manipulation of the local wettability of a surface by patterning it with hydrophobic and hydrophilic regions (that have significant difference in their intrinsic wettability) will result in preferential nucleation on the hydrophilic regions. These studies provide a pathway to better understand the fundamentals of heterogeneous nucleation of water and other areas such as ice formation and crystal nucleation.¹⁵ In contrast to the random nucleation behavior of superhydrophobic surfaces, textured hydrophobic surfaces with hydrophilic tops promote nucleation and growth of Cassie-type droplets and can therefore exhibit superior droplet shedding properties under condensation. As a result, these hybrid surfaces have a great potential to enhance condensation heat transfer¹⁶ and could broadly lead to efficient condensers in power generation and desalination, reduce moisture-induced efficiency losses in steam turbines, and enable high-performance heat pipes for electronics cooling applications.¹⁷

We thank Dr. M. Blohm and Nanotechnology Program of GE Research for support. We thank Dr. V. Smentkowski and Dr. S. Ostrowski for their help with ToF-SIMS. One of the authors (K.K.V.) acknowledges the support from d'Arbeloff Career Development Chair at MIT.

¹R. A. Sigsbee, in *Nucleation*, edited by A. C. Zettlemoyer (Marcel Dekker, New York, 1969).

²Y. T. Cheng and D. E. Rodak, *Appl. Phys. Lett.* **86**, 144101 (2005).

³Y. Zheng, D. Han, J. Zhai, and L. Jiang, *Appl. Phys. Lett.* **92**, 084106 (2008).

⁴R. D. Narhe and D. A. Beysens, *Phys. Rev. Lett.* **93**, 076103 (2004).

⁵K. A. Wier and T. J. McCarthy, *Langmuir* **22**, 2433 (2006).

⁶Y. C. Yung and B. Bhushan, *J. Microsc.* **229**, 127 (2008).

⁷C. Dorrer and J. Ruhe, *Soft Matter* **5**, 51 (2009).

⁸C. T. R. Wilson, *Philos. Trans. R. Soc. London, Ser. A* **189**, 265 (1897).

⁹See EPAPS supplementary material at <http://www.aip.org/pubservs/epaps.html>.

¹⁰A. Lafuma and D. Quere, *Nature Mater.* **2**, 457 (2003).

¹¹N. A. Patankar, *Langmuir* **20**, 7097 (2004).

¹²T. Deng, K. K. Varanasi, M. Hsu, N. Bhatte, C. Keimel, J. Stein, and M. Blohm, *Appl. Phys. Lett.* **94**, 133109 (2009).

¹³A. R. Parker and C. R. Lawrence, *Nature (London)* **414**, 33 (2001).

¹⁴L. Zhai, M. C. Berg, F. C. Cebeci, Y. Kim, J. M. Milwid, M. F. Rubner, and R. E. Cohen, *Nano Lett.* **6**, 1213 (2006).

¹⁵J. Aizenberg, A. J. Black, and G. M. Whitesides, *Nature (London)* **398**, 495 (1999).

¹⁶K. K. Varanasi, N. Bhatte, G. A. O'Neil, S. Ganti, J. Stein, T. Deng, N. A. Turnquist, M. K. Brun, F. Ghasripoor, K. Krishnan, and C. F. Keimel, U.S. Patent Application No. 20070028588 (2005).

¹⁷K. K. Varanasi and T. Deng, U.S. Patent Application No. 12/254561 (2008).